Vol. 48, No. 1 (2026) 1-20, DOI 10.24874/ti.1964.06.25.10

Tribology in Industry

www.tribology.rs

RESEARCH

Tribological Investigation of Automotive Brake Pad Friction Material Based on Rice Husk and Sugarcane Bagasse Ash

Sachin S. Barve[a,*], Hrishikesh Khairnar[a]

[a]*Veermata Jijabai Technological Institute (VJTI) , Mumbai, India.*

Keywords:

Asbestos
Copper-free
Fade
Recovery
SEM
EDX

* Corresponding author:

Sachin S. Barve
E-mail: ssbarve@me.vjti.ac.in

Received: 20 June 2025
Revised: 8 August 2025
Accepted: 3 October 2025

A B S T R A C T

The objective of this study has been to investigate the tribological performance of automotive brake pad friction material (BFM) made from agro-waste materials, specifically rice husk (RH) and sugarcane bagasse ash (SCBA). These materials were combined using phenolic resin along with other compositional components. The mechanical, physical, and tribological performance of both samples was assessed according to established standards. The microstructure of the samples was examined using Scanning Electron Microscopy (SEM) and Energy Dispersive X-ray Spectroscopy (EDX) to analyze the bonding and distribution of materials. The results indicated that sample 1 (S1) outperformed sample 2 (S2) in terms of compression strength, hardness, fade resistance, and recovery. The hot and cold coefficients of friction for sample 1 (S1) were 0.47 and 0.43, respectively, while for sample 2 (S2), they were 0.48 and 0.47. Chase test data revealed that both samples demonstrated a fade resistance of over 75% and a recovery exceeding 100%. The friction material was evaluated using edge code assessment, resulting in ratings of 'FG' for S1 and 'GG' for S2. The SEM-EDX analysis indicated that both samples had similar surface morphologies, and no fiber delamination was observed in either sample after the friction tests. This study adds to the growing body of research focused on developing safer and more environmentally friendly alternatives to traditional brake pad materials, which can be detrimental to the ecosystem.

1. INTRODUCTION

Automobiles utilize one of two primary brake system designs: disc brakes or drum brakes. Since ventilated brake discs are subject to varying loads, their design must provide satisfactory heat transfer and sufficient thermo-structural fatigue life. Therefore, they should be designed in accordance with coupled thermo-mechanical fatigue life. Currently, most cars are equipped with disc brakes due to their superior heat dissipation capabilities [1]. The type of

friction materials used significantly influences braking performance [2]. These friction materials consist of several unique fundamental components, including minerals, carbon, lubricants, metallic particles or fibers, as well as various abrasives and fillers, all bound together by a polymeric binder, typically a thermosetting polymer [3].

In the 19th century, "British Belting and Asbestos Limited" introduced asbestos-based brake pad materials because of their ability to dissipate excessive heat. Asbestos fibers have historically been valued for their exceptional mechanical and tribological properties, making them common additives in brake pad formulations integrated into polymeric matrices. [4] However, growing environmental and sustainability concerns have led to increased scrutiny of metallic and synthetic materials used in the braking industry. Consequently, non-toxic alternatives are gradually replacing hazardous substances like asbestos and copper previously used in brake friction materials (BFMs) [5]. Asbestos use is currently banned in over 60 countries [6-8].

Due to its harmful effects on aquatic life, the use of copper in BFMs has also been reduced and is limited to 0.5% in the United States by 2025. One of the most challenging tasks is replacing copper due to its significant impact on brake pad performance [6,8-9]. It is widely understood that substituting copper with a single ingredient can be difficult. Alternatively, brass can be employed as a critical component in brake pad formulations because it enhances thermal conductivity, wear resistance, fade resistance, and tribo-load bearing capacity. Research indicates that the solid lubrication and primary contact sites provided by brass fillers in brake pads act as reinforcing factors, facilitating smooth sliding behavior [10]. Furthermore, studies have shown that the tribological and physico-mechanical performance of brake friction materials (BFMs) is significantly influenced by the composition of brass, particularly the copper-to-zinc ratio [11]. Brass containing 80% copper and 20% zinc has been found to outperform other types of brass. Additionally, incorporating brass particles improves thermal characteristics and contributes to wear and friction mechanisms [12]. The friction coefficient stabilizes when there is an optimal amount of 4.5 weight percent of brass. However, it has also been observed that tribo-performance declines once the brass content exceeds the ideal value of 8% [13].
It has also been observed that the materials and design of brake pads have a big impact on how much noise they produce, which in turn affects the comfort and health of the rider [14]. Due to environmental concerns, conventional copper-based pads are being phased out. Fe–Al alloys, zinc, stainless steels, graphite/cellulose fibers, carbon fibers/nanotubes, and Promaxon-D fillers are some options that can lower noise without affecting braking performance. Formulations that are environmentally friendly (copper-free or asbestos-free) can still perform well in terms of tribological behavior and noise reduction [15].

The adverse impacts of asbestos and copper on the environment and humans have spurred interest in natural compounds as potential substitutes for the toxic materials used in BFMs. These natural substances are plentiful and possess favorable mechanical and physical properties, offering numerous advantages. Researchers have made several attempts to utilize organic and agricultural waste to develop non-asbestos friction materials [16-17]. Various friction materials have been created using pineapple [18], kenaf [19], palm kernel shell (PKS) [20,21], flax [22], bamboo [23], abaca [24], hemp [25], coconut (coir) [26], jute, ramie, sisal [27], corn husk [28], banana [29] , sugarcane bagasse [30], rice husk [31], and their derivatives [32].

India plays a significant role in the global agricultural economy, with approximately 70% of its population relying on farming for their primary source of income. The country ranks among the top two producers of rice and sugarcane (refer Figs. 1 and 2) [33]. This substantial agricultural output generates a considerable amount of waste, including crop residues. Some of this waste finds use as cattle feed, fuel for burning, or in the production of by-products, but a significant portion remains unused [34-35].

Farmers commonly burn agricultural leftovers in open fields to dispose of this waste. This practice releases a significant amount of pollutants into the air, negatively impacting public health [36].

Air pollution is the second leading cause of health issues in South Asia. It can result in various problems affecting the skin, eyes, lungs, heart, and nervous system [37]. Elevated levels of air pollution can lead to conditions such as asthma, bronchitis, chronic obstructive pulmonary disease (COPD), reduced lung capacity, emphysema, cancer, and other long-term health complications. Therefore, it is crucial to identify efficient methods to utilize this agricultural waste productively and mitigate environmental pollution [38].

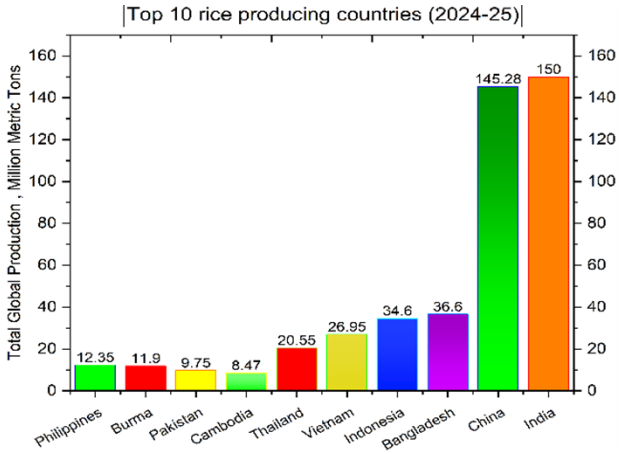

Fig. 1. Rice production in India (2024-25) [39].

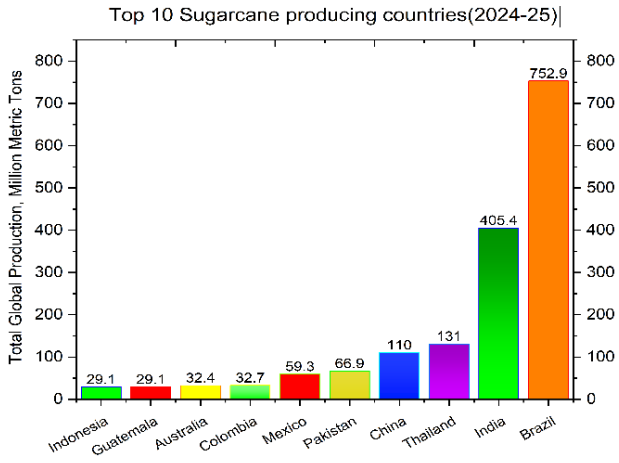

Fig. 2. Sugarcane production in India (2024-25) [40].

While examining organic and agricultural wastes, rice husk and sugarcane bagasse (refer to Table 1) emerge as notable natural constituents. This is attributed to their high ash concentration, primarily composed of amorphous silica, which results from thermal degradation [41].

Air pollution originates from both natural sources and human activities. Recently, it has been projected to be a leading cause of approximately seven million deaths. Vehicles are now recognized as the primary source of particles released to the environment. The main contributors to particulate emissions from cars include engine fuel combustion, the wear debris of friction components such as brakes and clutches, and tire degradation. The wear products generated in the braking system are complex, as brake pads consist of various materials. Many earlier studies on organic materials did not measure particulate matter (PM) emissions, leading to inaccurate assessments of their methodologies [42,43].

Table 1. Ash and silica content of plants [41].

Plant	Parts of the plant	Ash (%)	Silica (%)
Sorghum	Leaf sheath epidermis	12.55	88.7
Wheat	Leaf sheath	10.48	90.56
Corn	Leaf blade	12.15	64.32
Bamboo	Nodes (inner portion)	1.49	57.4
Bagasse	--	14.71	73
Lantana	Leaf and stem	11.24	23.28
Sunflower	Leaf and stem	11.53	25.32
Rice husk	---	22.15	93
Rice Straw	----	14.65	82
Breadfruit tree	Stem	8.64	81.8

When inhaled frequently and over prolonged periods, crystalline silica is classified as hazardous by the International Agency for Research on Cancer (IARC). It has been listed as a carcinogenic agent in Group 1. In contrast, amorphous silica is not deemed to be hazardous to humans, as it falls under IARC Group 3 [44]. Some studies suggest that amorphous silica may have certain adverse health effects. However, they are not considered as severe as those associated with crystalline silica. Particularly at elevated temperatures, the silica content can significantly enhance friction performance [32,45]. Additionally, the hardness properties of silica contribute to the exceptional mechanical capabilities of brake composite materials. It has also been revealed that temperature significantly affects the structural and contact behaviour of disc brakes. So, it is essential to recognize that both rice husk and sugarcane bagasse, as agro-industrial waste, present viable alternatives [46].

Considering the benefits of rice husk (RH) and sugarcane bagasse (SCBA), along with the drawbacks of asbestos and copper, this study demonstrated the feasibility of using a combination of RH and SCBA in brake friction materials (BFM), providing an eco-friendly alternative to traditional materials. Additionally, copper has been effectively replaced by brass in this application. The composition is detailed in Table 2. The samples were tested for the coefficient of friction (COF) using various friction test setups, viz., a pin-on-disc tribometer and a friction test rig. Furthermore, the thermal degradation of the samples was assessed through thermogravimetric analysis, yielding promising results emphasizing the advantages of reusing agricultural waste in industrial applications [47].

However, for better understanding of the tribological behaviour of BFM, fade and recovery performance and the worn-out surface morphology are also important. In previous studies of BFM that utilized a combination of rice husk (RH) and sugarcane bagasse ash (SCBA), these crucial tribological investigations were not conducted.

Therefore, the objective of this study has been to evaluate the tribological performance of BFM developed with RH and SCBA by performing fade and recovery tests and microstructural analysis. The Chase test has been conducted in accordance with the IS:2742/1994 (SAE J661) standard to assess fade and recovery performance, while scanning electron microscopy (SEM) and energy dispersive X-ray (EDX) microanalysis were employed to examine the wear characteristics of the brake pad material.

2. MATERIAL DEVELOPED

All ingredients have been weighed on a scale according to the specified composition (refer to Table 2). They were mixed in a ball-type mixer for 30 minutes at a speed of 100 rpm. Different weight percentages of rice husk and sugarcane bagasse ash were incorporated into the mixture to create two distinct formulations. While S1 contains 6% RH and 5% SCBA, S2 includes 5% RH and 6% SCBA. The remaining ingredients remained constant. The samples were made using standard practices of hot compression moulding and then cured in a furnace at the specified pressure and temperature. The moulding and curing parameters are presented in Table 3. Initially, the samples were formed into square sheets measuring 500 x 500 x 10 mm in thickness and were subsequently finished to the required specimen size (refer to Figs. 3a and b).

Table 2. Formulation for brake pad friction material (% by weight).

Ingredient	S1	S2
Binder: Phenolic resin	20	20
Filler: Sugarcane bagasse ash, Calcium carbonate, China clay, Magnesium oxide, Barium sulfate, Carbon powder, Coke powder grit 40, NBR powder	45	46
Friction modifier: Rice husk, Friction dust, Wollastonite, Red and Yellow oxide	19	18
Lubricant: Graphite fine (95% purity synthetic)	2	2
Reinforcement: Brass, Alumina, Glass fiber (4 mm, 6 mm)	14	14

(a)

(b)

Fig. 3. Fabricated samples – (a) S1, (b) S2.

Table 3. Manufacturing parameters.

Parameter	Values	
	S1	S2
Moulding time (min.)	15	15
Moulding Temperature, Average (deg C)	120	120
Moulding Pressure (bar)	350	300
Curing time (min.)	12	12
Curing Temperature (deg C)	100-110	100-110
Curing Pressure (bar)	300	280

3. MATERIAL CHARACTERIZATION

3.1 Mechanical and physical test

The standard procedure was employed for both samples to determine the density and hardness by following IS2742/2014 part 3 and IS2742/1994, respectively. Testing in accordance with ASTM D 6641-2023 has been conducted to ascertain the maximum force and compression strength. The crosshead speed and grip separation were set at a rate of 0.05 inches per minute. The average sample size was 5.31 mm thick and 26.53 mm wide. Tension tests were carried out according to ASTM D3039-2014, resulting in the determination of ultimate tensile strength and breaking stress. The rate of grip separation/crosshead speed was 2 mm/minute, with a preload of 0.1 MPa. The average sample size for these tests was 5.40 mm thick and 25.97 mm wide. Lateral shear strength has been calculated following ASTM D3518-2018, which included the assessment of in-plane shear strength and force at failure. The crosshead speed and grip separation rate for this test were 0.02 inches/minute, with a preload of 0.5 MPa. The average sample size was 5.40 mm thick and 26.72 mm wide. Three-point bending flexural tests have been performed in compliance with ASTM D790-2017 to measure flexural strength and flexural modulus. The rate of grip separation/crosshead speed was set at 1% per minute, and a preload of 0.2 MPa was applied. The average sample size for the bending tests was 5.31 mm thick and 26.01 mm wide, conducted using a span of 84.8 mm. The results are discussed in the following section.

3.2 Fade and recovery test

The fading phenomenon indicates a deviation from the friction law in friction materials, which adversely affects brake effectiveness and reliability. High temperatures at the contact point between the braking disc and pad reduce the brake pad's shear strength, thereby diminishing frictional force and leading to fade. The material determines the ideal operating temperature for maximum friction and the critical temperature for brake fade [48]. Too much cooling prevents the pad from reaching its best temperature, whereas inadequate cooling can cause fading. In both of these cases safety is compromised by taking longer stopping distances [49].

Friction performance, or fade performance, at elevated temperatures is commonly used to evaluate friction materials. For the experiments conducted on the Chase test setup, samples measuring 25x25x5 mm were prepared. The tests were performed according to the IS2742/1994 (SAE J661) standard. A cast iron drum with a diameter of 279 mm was utilized, rotating at a speed of 411 rpm. A normal load of 67 kg was applied to the sample. The testing process followed the schedule outlined in IS2742/1994, as shown in Table 4.

Table 4. Test Schedule as per IS2742 [51].

Sr. No.	Test name	Speed (rpm)	On time		Off time	No. of brake applications	Temperature (^{o}C)	Heater	Blower
			Min	sec	sec				
1	Burnishing (20 min)	308	20	-	-	1	-----	Off	Off
2	Baseline-1	411	-	10	-	20	82–104	Off	Off
3	Fade-1	411	10	-	-	1	82–289	On	Off
4	Recovery-1	411	-	10	-	1	261–82	Off	On
5	Wear	411	-	20	10	100	188–195	Off	Off
6	Fade-2	411	10	-	-	1	82–345	On	Off
7	Recovery-2	411	-	10	-	1	317–82	Off	On
8	Baseline-2	411	-	10	20	20	82–104	Off	Off

Following coefficients of friction (COF) and tribological performance data have been estimated [10].

1. COF minimum: This is the lowest COF for cycles of recovery, fade, and cold.
2. COF maximum: This is the highest COF for cycles of cold, fade, and recovery.
3. COF Performance: This represents the average COF for cycles of fading and recovery.
4. COF Fade: This is the associated fade cycle's minimum COF.
5. The maximum COF for the relevant recovery cycle is COF Recovery.

From the above-mentioned values of COF, the fade resistance and recovery data obtained are as follows:

$$\% \text{ Fade resistance} = \frac{\text{COF Fade}}{\text{COF Performance}} \text{ x } 100 \quad (1)$$

$$\% \text{ Recovery} = \frac{\text{COF Recovery}}{\text{COF Performance}} \text{ x } 100 \quad (2)$$

To evaluate the coefficient of friction (COF) for both samples, the Edge code serves as a reference. Edge ratings are represented alphabetically, beginning with the letter 'C' for the lowest friction. As you progress down the alphabet column, the friction levels increase. These ratings are detailed in Table 5. To identify the COF for each entry, two consecutive letters are required. The first letter indicates normal friction, while the second letter denotes hot friction [50].

Table 5. Rating of brake pad [50].

Rating	Coefficient of Friction
C	Not over 0.15
D	Over 0.15 but not over 0.25
E	Over 0.25 but not over 0.35
F	Over 0.35 but not over 0.45
G	Over 0.45 but not over 0.55
H	Over 0.55

3.3 Microstructural analysis

The compositions and morphologies of the composite surfaces have been examined using Energy Dispersive X-ray Spectroscopy (EDX) and Scanning Electron Microscopy (SEM). The contact area on the composite surface plays a crucial role in defining the friction characteristics. SEM and EDX proved to be powerful analytical techniques for structural and elemental analysis across various materials. SEM provides high-resolution images of the sample's surface morphology, while EDX determines the elemental composition [52].

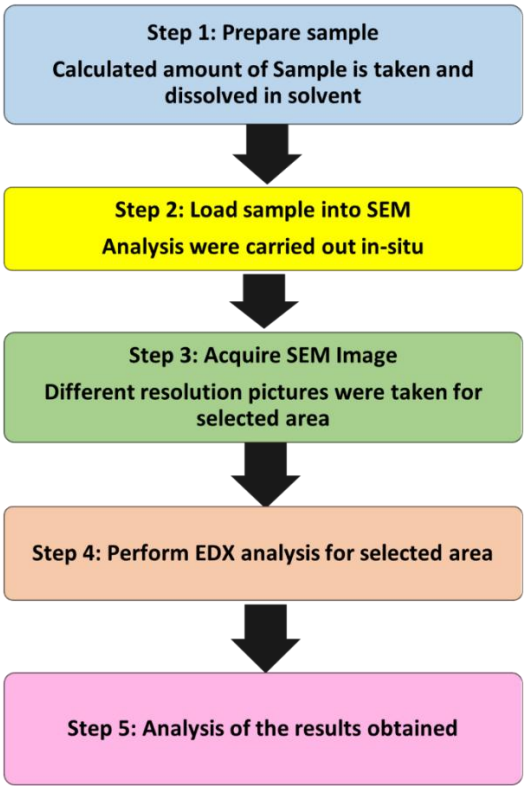

Fig. 4. Flowchart showing steps in SEM EDX analysis.

A simple flowchart is shown in Fig. 4. The steps followed for SEM/EDX analysis are:

1. Clean, stabilize, dehydrate, and mount the sample on a stub. If needed, next coat it with a conductive substance.
2. Put the sample into the SEM vacuum chamber with the high vacuum turned on.
3. Select the appropriate Secondary Electron (SE) detector.
4. After adjusting the height, focus on the sample, capture high-resolution SEM images, and use the EDX detector simultaneously to analyze and map the sample's elemental composition.

In this study, SEM and EDX microanalysis have been employed to investigate the surface morphology of the brake pad material in detail. The analysis of S1 and S2 has been carried out before and after the friction test to assess the wear performance.

4. RESULTS AND DISCUSSION

The density of commercial brake pad friction material typically ranges between 1.01 and 2.06 gm / cc. The recorded densities for S1 and S2 were 2.00 and 1.98 g/cm^3, respectively, which falls within the acceptable range for commercial pads [53,54]. While a lower-density brake pad material is generally preferred due to its lighter weight and reduced mass, the increased density observed in these samples [55]. This value is primarily attributed to a higher filler content, which enhances the homogeneity of the composite brake pads. Additionally, compared to sugarcane bagasse ash, rice husk (RH) contains a greater proportion of amorphous silica. The amorphous silica particles fill the voids within the mixture, contributing to the overall density. Other organic constituents in RH, such as hemicellulose and lignin, further contribute to the increased density [54].

An optimal composition for brake pad friction material is expected to yield hardness values ranging from 70 to 100. In contrast, commonly used asbestos-based brake pad materials have a hardness of approximately 101 HRB [3]. The measured hardness values fall well within the range of hardness values required for brake pad material [21]. The hardness values measured for both samples are well within the necessary range for brake pad materials. Although both samples have the same proportion of phenolic resin, S1 exhibits a higher hardness than S2, indicating that particle bonding is more effective in S1. Furthermore, the increased molding pressure may also have influenced the hardness of S1.

The literature indicates that brake pad compressive strength typically ranges from 70 to 125 MPa, based on the specific formulation and type of brake pad. While both samples fall within this range, their compressive strengths are lower than those of commercial brake pads [56,57]. This difference can be attributed to the larger particle size of the rice husk used in the samples. Research showed that reducing particle size enhances compressive strength. S1 exhibits a higher compressive strength compared to S2, likely due to its greater density (refer to Figs. 5 a and b) [58,59].

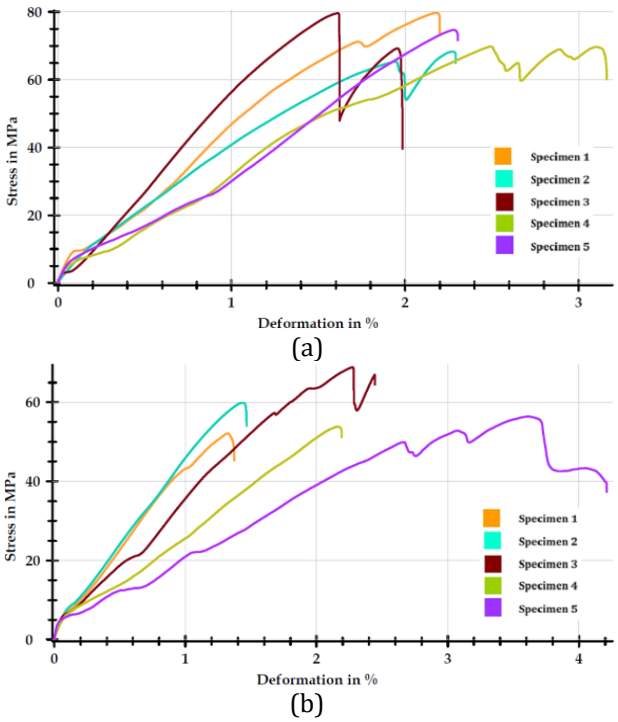

Fig. 5. Compression test results for a) S1 and b) S2.

The shear strength of commercial brake pads, which are made of asbestos, is reported to be 5.46 MPa [60]. S1, containing a higher weight percentage of rice husk, exhibits a lower shear strength compared to a commercial brake pad. Conversely, S2 contains a greater weight percentage of sugarcane bagasse ash (SCBA), which enhances the connection between the particles and the binder during the molding process (refer to Figs. 6 a and b).

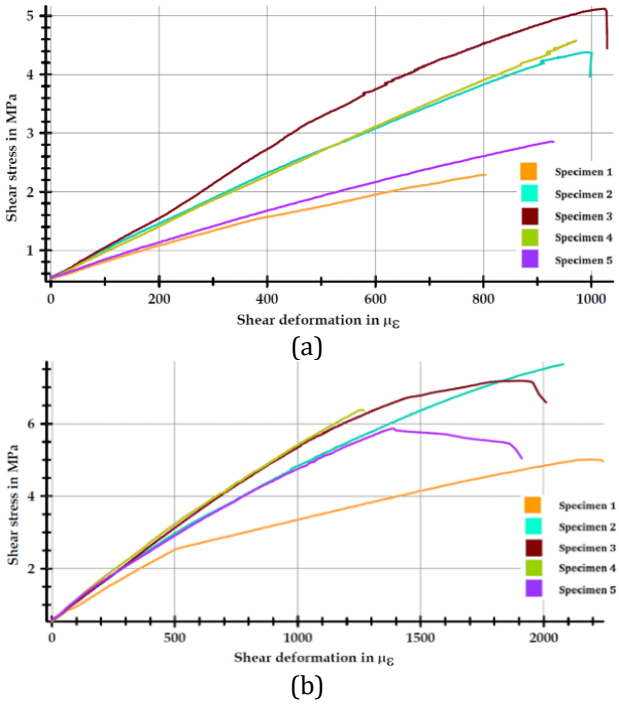

Fig. 6. In-plane shear test results for a) S1 and b) S2.

The tensile strength of a commercial brake pad is approximately 7.0 MPa [61]. Both samples demonstrate tensile strengths that are comparable to that of commercial brake pads (refer to Figs. 7 a and b). Research indicates that brake pads generally have a flexural strength ranging from 10 to 40 MPa [62]. The specific strength values depend on various factors, including the production procedure, bonding, reinforcements, and material composition. Both samples exhibited strengths within this range (refer to Figs. 8 a and b). The mechanical test comparisons are illustrated in Fig. 9, showing that S1 outperforms in terms of compressive strength and hardness, while S2 excels in tensile strength and in-plane shear strength. A comparison of the physical and mechanical properties of S1 and S2 with relevant materials available in the literature, as well as with commercial brake pad materials, is presented in Table 6.

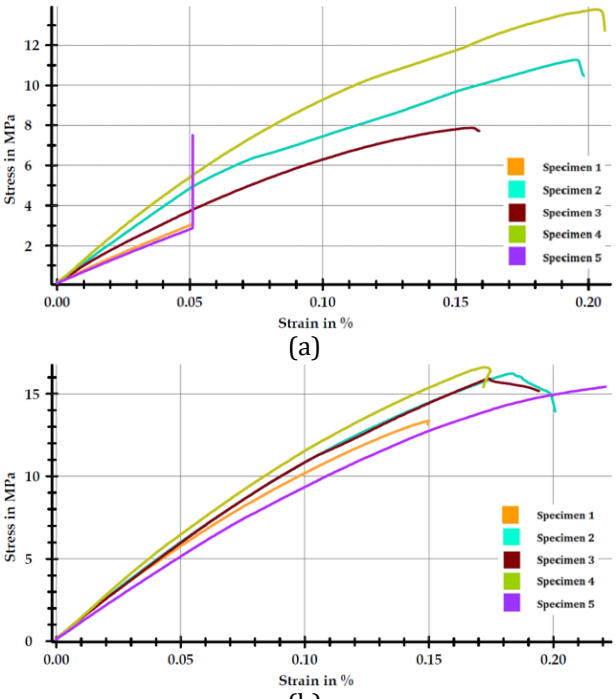

Fig. 7. Tension test results for a) S1 and b) S2.

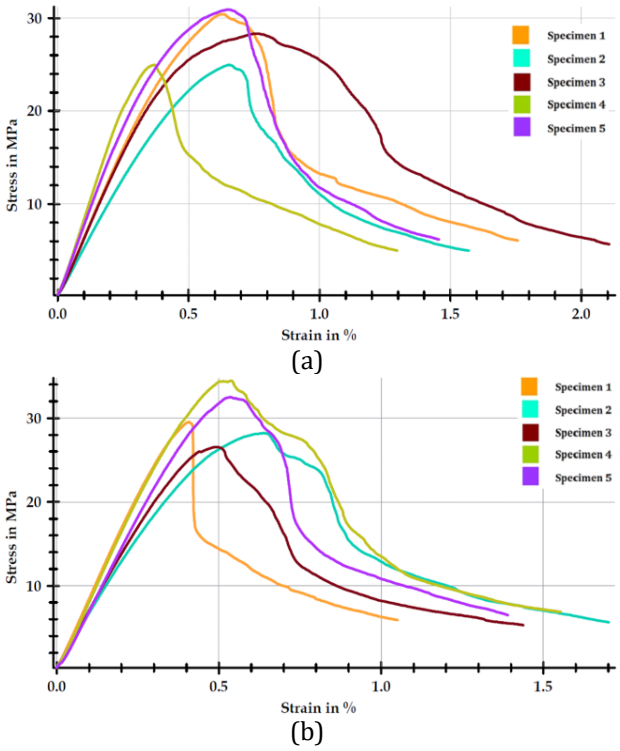

Fig. 8. Flexural test results for a) S1 and b) S2.

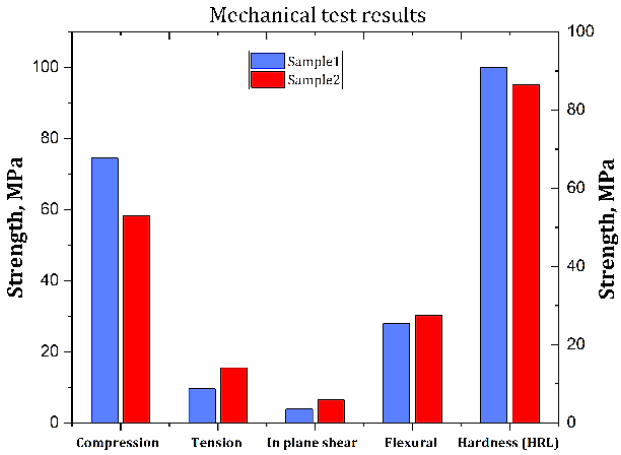

Fig. 9. Consolidated results of mechanical test results for S1 and S2.

Table 6. Comparison of physical and mechanical test results with other comparable materials.

Brake pad material	Property						Reference
	Density (gm/cc)	Hardness	Compression strength (MPa)	Tensile strength (MPa)	In-plane shear strength (MPa) at failure	Flexural strength (MPa)	
Sample 1	2.00	100 HRL	74.42	9.58	3.85	27.91	---
Sample 2	1.98	95 HRL	58.21	15.50	6.41	30.25	---
Commercial Brake Pad (Asbestos-based)	1.89	101 HB	110	--	5.46	---	[21]
Palm Kernel Based	1.65	92 HB	103.5	--	--	--	[21]
Banana peel	1.26	98.8 HB	95.6	--	--	--	[29]
Bagasse based	2.1-2.5	100.5 HB	105.6	13 - 25	--	51 - 83	[30]
Rice husk based	1.96-2.08	68-85 HRR	--	--	--	--	[31]

4.1 Fade and recovery

Fade and recovery performance are commonly used to demonstrate the temperature-dependent sensitivity of the coefficient of friction (COF) in friction materials. Recovery refers to the regaining of original performance under normal conditions, while fade is related to the decline in COF that occurs at elevated temperatures.

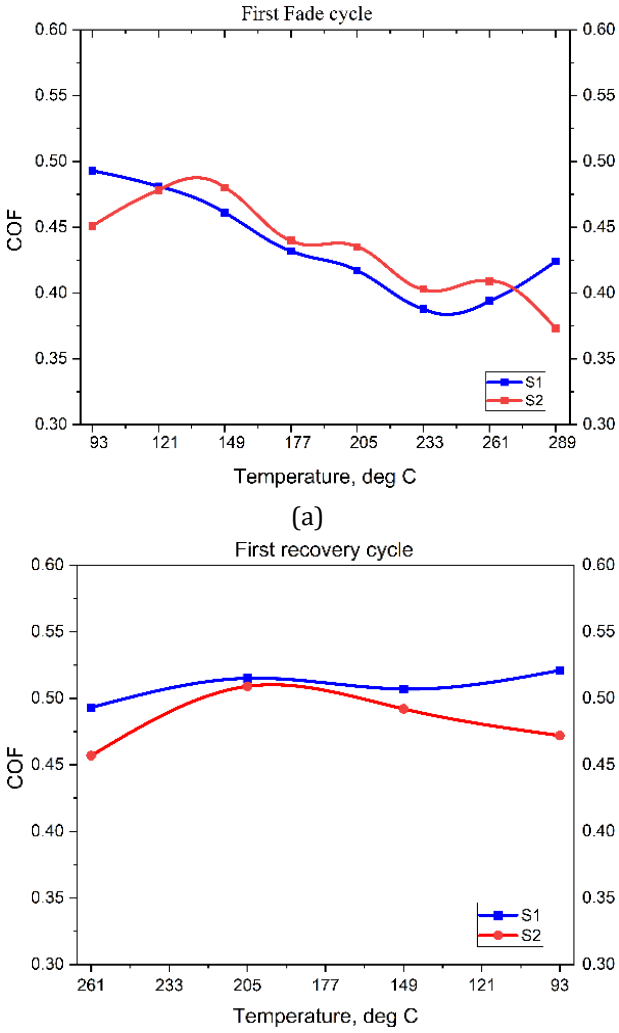

Fig. 10. COF variation for S1 and S2 during the first a) fade cycle and b) recovery cycle.

The results from the Chase test are presented in fig. 10 and 11, illustrating the fade and recovery characteristics for both samples. As shown in Fig. 10 a, the performance of the friction composites did not follow a distinct trend. At the initial temperature of 93°C during the first fade cycle, the friction coefficient (COF) values for all samples remained within the desired range of 0.3 to 0.7, typically expected for brake lining materials [63]. The fade COF for S1 and S2 at this level was 0.39 and 0.37, respectively, indicating minimal difference between the two. After exposure to a temperature of 289°C, there was still no significant change in their performance order, with COF values consistently in the range of 0.3 to 0.7. Following a 10-minute run at 288°C, the COF remained above 0.35.

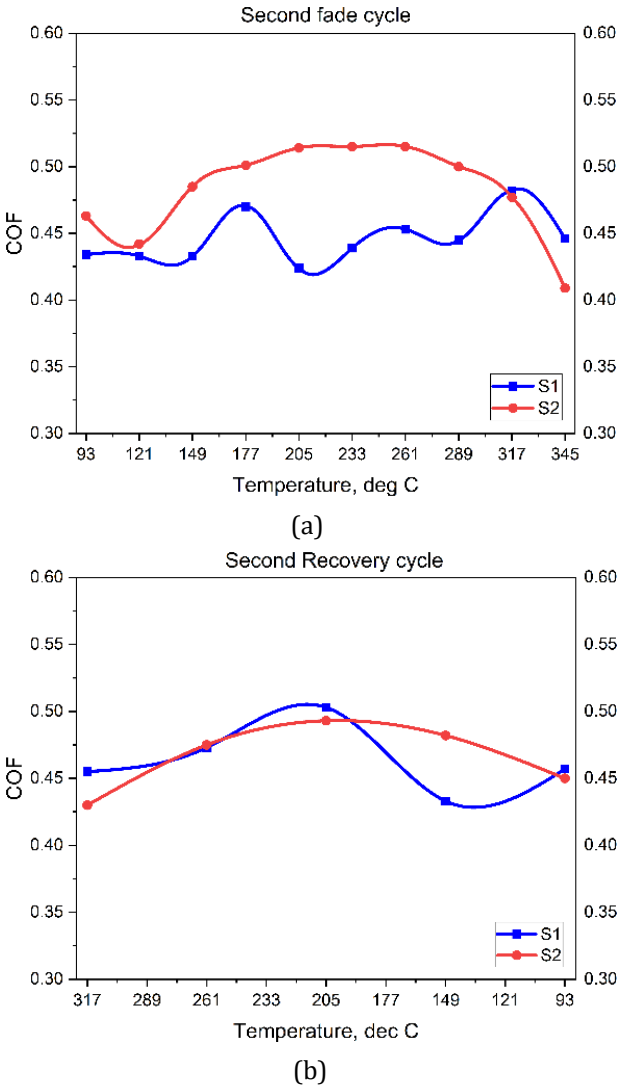

Fig. 11. COF variation for S1 and S2 during the second a) fade cycle and b) recovery cycle.

During the first recovery cycle, a general improvement in COF was observed as the temperature decreased from 261°C to 93°C; S1 demonstrated higher performance than S2, with recovery COF values of 0.521 for S1 and 0.509 for S2 (refer to Fig. 10b).

In the second fade cycle, as the temperature rose to 345°C, another shift in the derived COF was noted. While S1 showed minimal variation, S2 experienced significant changes in COF. The fade

COF during this cycle was nearly identical, measuring 0.42 for S1 and 0.41 for S2. The COF in this cycle has shown some improvement compared to the first fade cycle (refer to Fig. 11a).

At the conclusion of the second recovery cycle, both S1 and S2 maintained their relative positions despite a slight decrease in COF compared to the first recovery cycle (refer to Fig. 11 b). The recovery COF for this cycle was recorded at 0.503 for S1 and 0.493 for S2. Throughout the entire fade and recovery test, the COF never fell below 0.3, which is the minimum requirement for effective BFM. The observations from the Chase test are outlined in Table 7 as follows.

Table 7. COF from fade and recovery test.

Parameter	S1	S2
Performance COF	0.46	0.46
COF - Fade 1	0.39	0.37
COF - Recovery 1	0.521	0.509
COF - Fade 2	0.42	0.41
COF - Recovery 2	0.503	0.493

The percentage of fade resistance and recovery has been calculated, following the discussion in the previous section, and it is presented in Table 8. A fading rate of less than 25% (indicating a fade resistance greater than 75%) is considered a critical safety criterion for braking, as fading friction becomes particularly significant at any given speed during continuous deceleration [3].

Table 8. % Fade resistance and % recovery.

	S1	S2
% Fade 1 resistance	84.78	80.43
% Fade 2 resistance	91.30	89.13
% Recovery 1	113.26	110.65
% Recovery 2	109.34	107.17

It is observed from Fig. 12 that both samples exhibit fade resistance exceeding the required threshold. However, S1 demonstrated slightly superior performance compared to S2. The primary cause of fading is the thermal breakdown of organic components, which occurs due to heat accumulation at the contact point [64]. The material loss and degradation of S1 is less pronounced than that of S2 at approximately 350°C, resulting in better fade performance for S1 [47]. The recovery rate is a crucial factor influencing the friction value. Typically, the recovery rate of brake pad materials is expected to fall between 75 and 100 percent [65]. Fig. 13 illustrates that the recovery characteristics of both S1 and S2 are comparable.

In both fade cycles, the coefficient of friction (COF) exceeds 0.35, while the general requirement for COF during fade is between 0.35 and 0.45 [10]. Throughout the fade and recovery cycles, the COF remains consistently between 0.3 and 0.7, which represents the typical range for motor vehicles in the market.

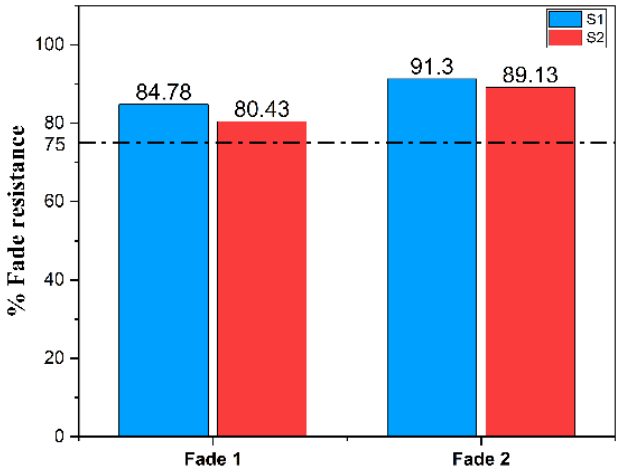

Fig. 12. Percentage Fade resistance of S1 and S2.

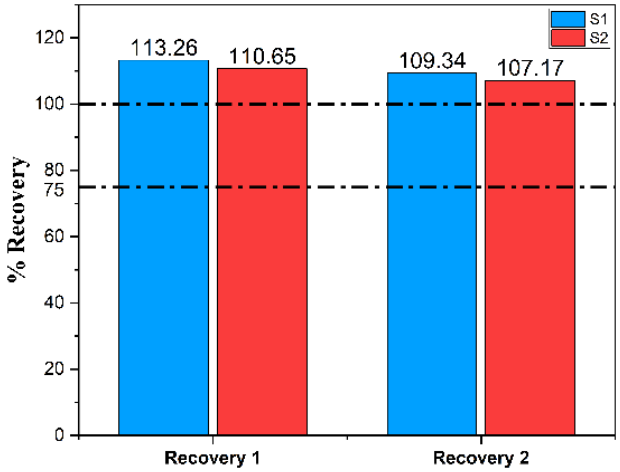

Fig. 13. Percentage Recovery of S1 and S2.

The wear behavior is a critical and changing property that is closely related to the material's thermal characteristics and the conditions in which it is used. According to the Chase test data, the wear mass percentages for S1 and S2 were calculated at 11.32 and 11.11, respectively [66]. Although S1 exhibits greater hardness, its wear is slightly higher than S2, as indicated in Table 9.

Table 9. Wear test data.

	S1		S2	
	Mass (gm)	Thick (mm)	Mass (gm)	Thick (mm)
Initial	6.89	4.19	6.84	4.09
Final	6.11	3.7	6.08	3.58
Wear loss	0.78	0.48	0.76	0.51
Wear %	11.321	8.03	11.111	8.43

This discrepancy can be attributed to the fact that as speed and load increase, the wear values also rise. The repetitive impact loading caused by the asperities on the counter face escalates with sliding speed. This increase in frictional thrust accelerates the debonding and fracture of the reinforcing fibers, leading to chattering and localized vibrations at the sliding surface. Consequently, these fibers may negatively affect the counter-face film, thereby increasing the specimen's wear rate [67].

4.2 SEM and EDX study

EDX and SEM were utilized to conduct a comprehensive examination of the wear mechanism in the brake pad material. The analysis of S1 and S2 was performed to evaluate their wear performance. Observations using SEM, EDX, and mapping were made before and after the friction test on the actual brake pad friction material for S1 and S2 (refer to Figs. 14 and 15).

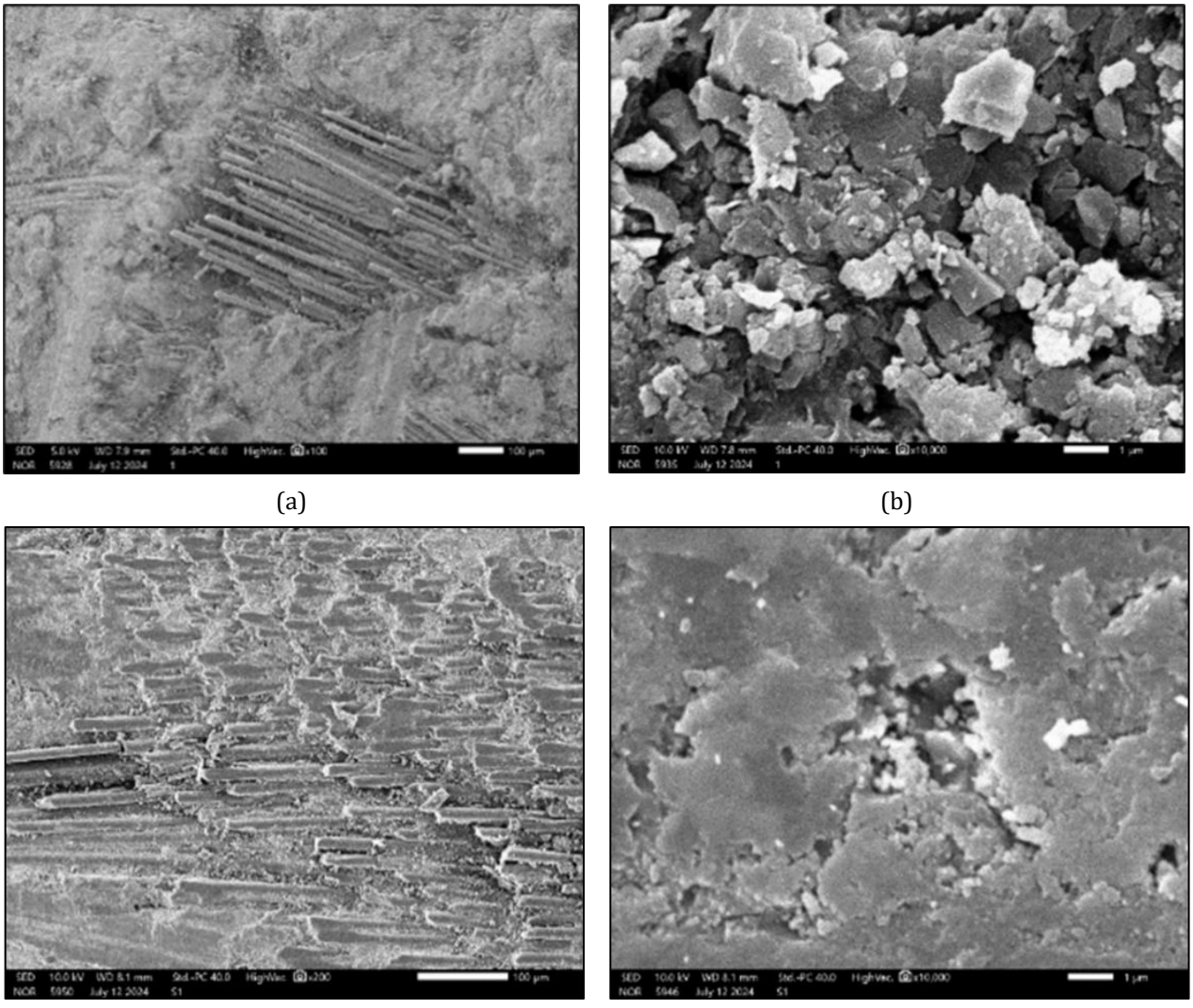

(a) (b) (c) (d)

Fig. 14. SEM Images of S1- a) and b) before the friction test, c) and d) after the friction test.

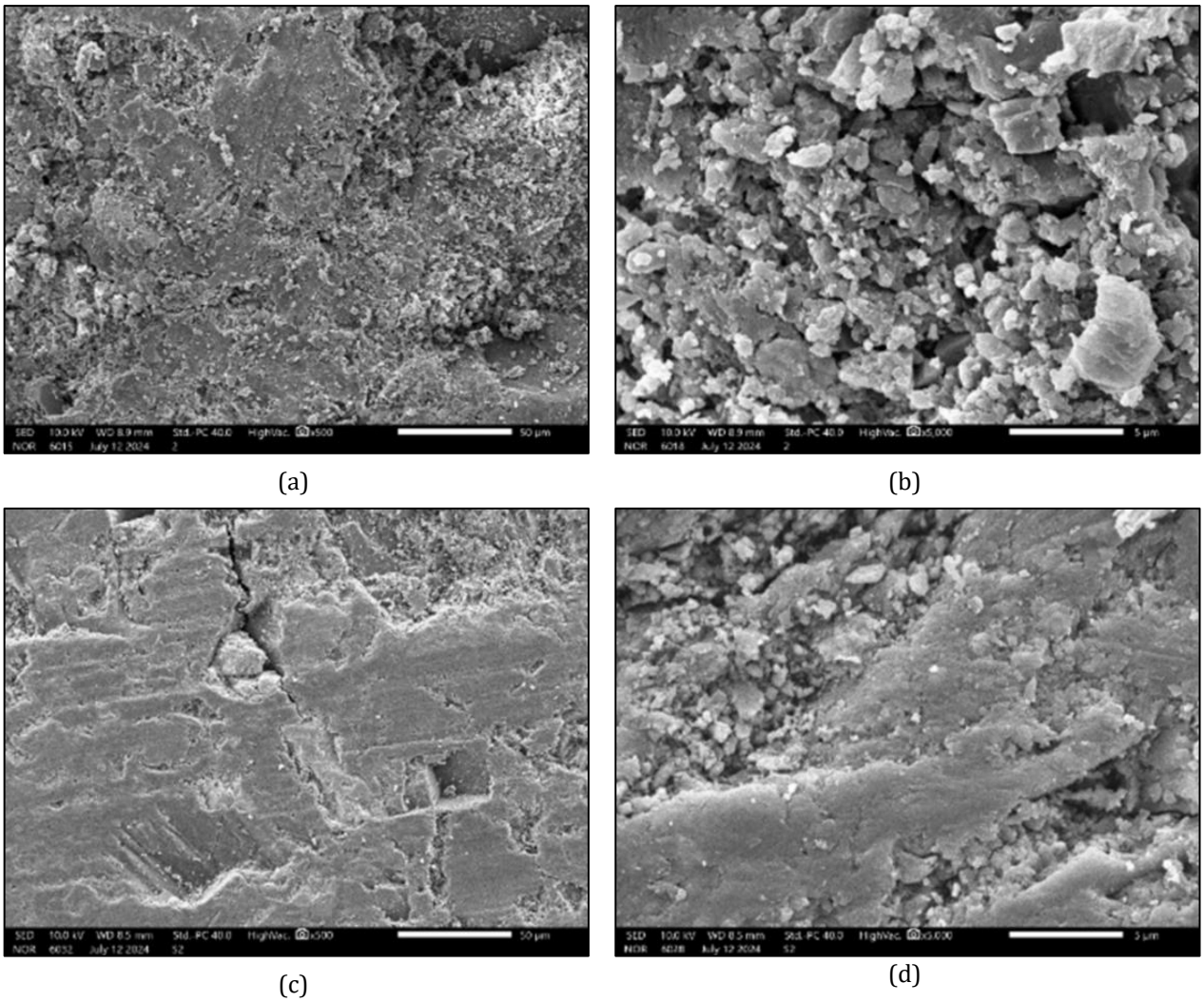

Fig. 15. SEM Images of S2– a) and b) before the friction test, c) and d) after the friction test.

Figs. 16 a) and b) present the SEM analysis of S1 and S2, respectively, captured at the micro scale prior to testing. The white spots and black regions observed in fig. 16 a) for S1 indicate the homogeneity of the sample. The area marked by the red circle highlights the uniform flat surface of the braking pad, along with the material's composition (see Fig. 16 a). The elemental composition of S1 before testing is also detailed, confirming that all components used in the pad material are present in the analysis.

Fig. 16 b) illustrates the microstructure of S2 before its use. The surface morphology of the S2 demonstrates that the majority of the pad's surface is uniformly covered by the composite material. The red circle in Fig. 16 b) indicates the presence of some voids in the material, attributed to the filler material in the braking pad composition. Overall, the S2 exhibits greater uniformity compared to the S1 at the micro-scale [68,69].

The SEM-EDX analysis reveals that various components contribute to the composition of the brake pad. The elemental makeup of S1 and S2 before use is presented in Table 10.

Table 10. Weight percentage composition of S1 and S2 before the friction test.

S1 Before test			S2 Before test		
Element	**Weight %**	**Atomic %**	**Element**	**Weight %**	**Atomic %**
C K	41.1	54.2	C K	35.5	48.4
O K	36.5	36.1	O K	38.1	39
MgK	1.6	1.1	MgK	1.7	1.2
AlK	4.2	2.5	AlK	4.1	2.5
SiK	7.8	4.4	SiK	11.1	6.5
MoL	5	0.8	MoL	3.2	3.1
CaK	1.9	0.8	CaK	4.1	2.9
BaL	1.8	0.2	BaL	2	11.7
			FeK	0.2	17.3

The analysis indicates that the percentage of oxygen (O) elements in both samples is nearly identical (refer to Figs. 16 a and b). This observation suggests that the unprocessed components consist of oxides, including common types such as magnesium oxide, zinc oxide, iron oxide, and aluminium oxide. These oxides serve as abrasive agents to enhance the friction level of the brake pads [70]. Often, these abrasive materials are incorporated into the pads to improve the coefficient of friction of the brake friction material (BFM).

Additionally, the highest concentration of carbon (C) and the lowest concentration of magnesium (Mg) in the material imply the presence of rice husk, sugarcane bagasse ash, and fine graphite. This observation supports the use of graphite as a lubricant during the manufacturing process [52].

A constant degree of friction is maintained by the lubricating chemicals, which also lessen the wear of the friction material. The EDX examination reveals the presence of the element Fe. It showed that steel fibers are present, which raises the voids and coefficient of friction. CA stands for calcium carbonate, which is utilized in S1 and S2 as a gap filler. The stable friction layer in brake pads is maintained by the Si, Mo, Ba, and Fe acquiring weights [53,71,72].

Lastly, the EDX examination of the element's composition, displayed in Figs. 16 and 17, showed that various calcium carbonates and carbon and oxide compounds constitute the majority of its contents. Nevertheless, the EDX analysis only reveals the chemical makeup of the composite material at some locations; it is not a reliable way to assess the chemical makeup of the sample's entire surface. Areal chemical analysis is suggested by the mapping composition as a means to have a better understanding of the pad's chemical behavior in these types of braking applications [73,74].

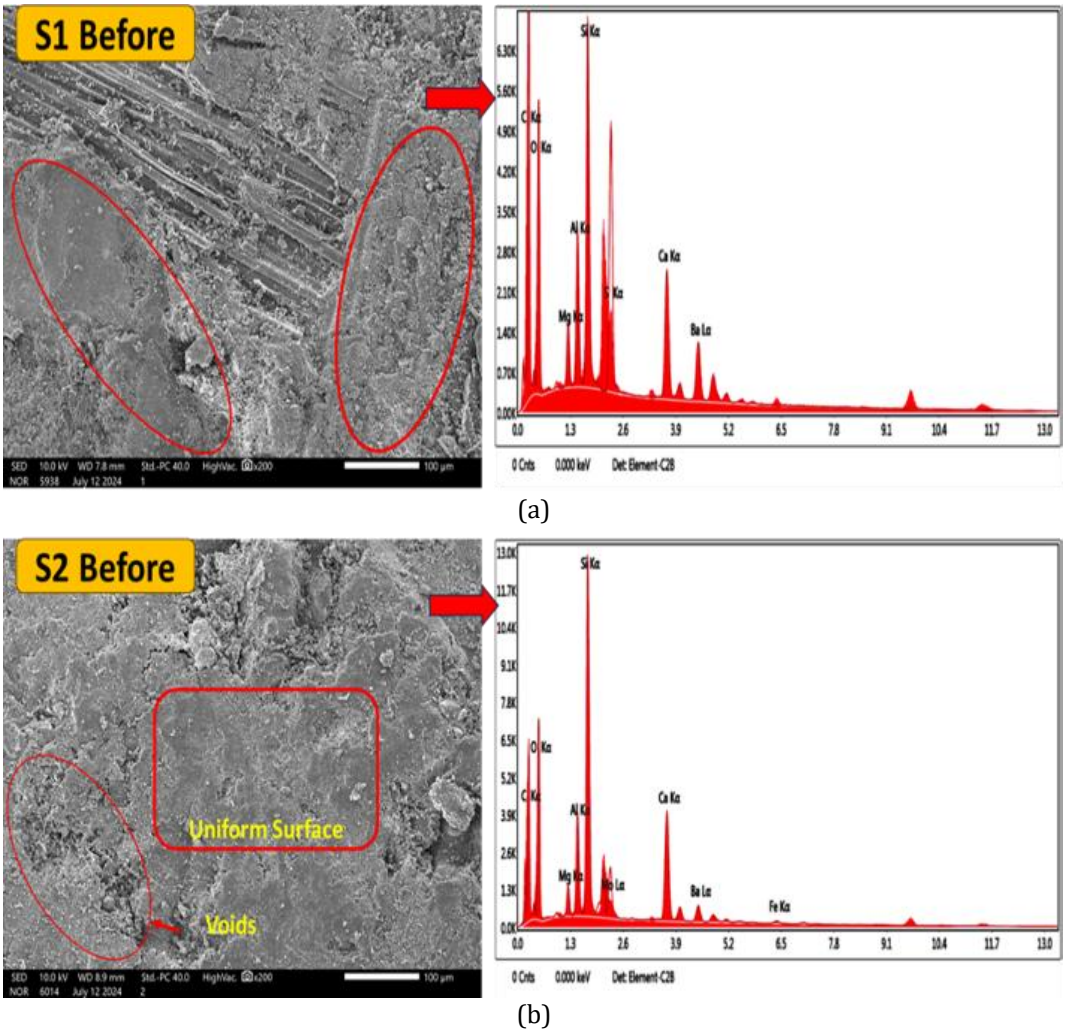

(a)

(b)

Fig. 16. SEM and EDX observation before friction test for fabricated a) S1 and b) S2.

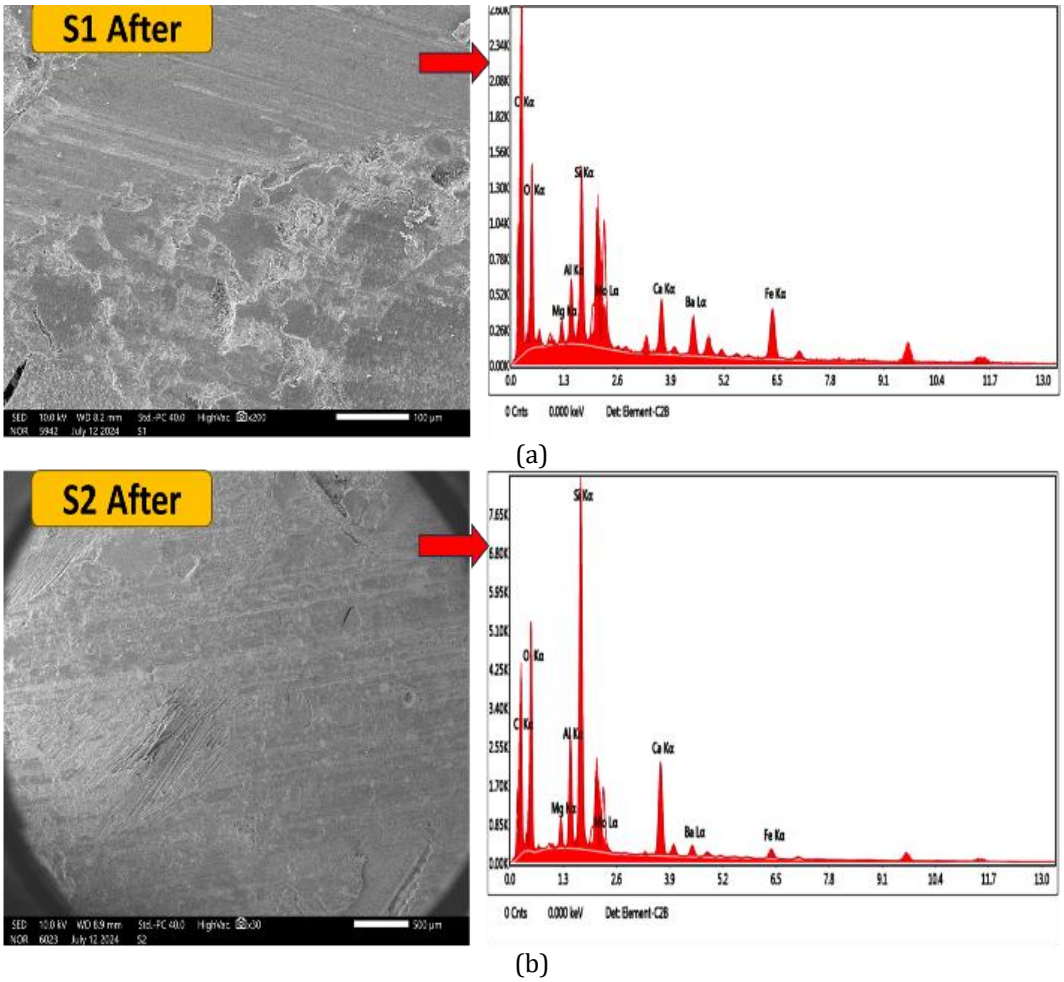

Fig. 17. SEM and EDX observation after friction test for a) S1 and b) S2.

The SEM analysis images of S1 and S2 at the micron scale following service are displayed in Fig. 17 a) and b), respectively. After service, cracks are visible at the bottom left of the lining in Fig. 17, indicating rust formation due to friction. The directions of the friction traces are also identified. Fig. 17 illustrates the wear modes observed. Notably, neither sample shows any fiber delamination after service. Both samples demonstrate satisfactory performance against brake pad wear, with the matrix effectively holding the composition and resisting material friction. A common wear mode observed when hard pad particles interact with the disc surface is known as abrasive wear [75,76].

There are no micro-cracks observed in the radial direction on the surface of the pads. However, the surface of sample S2 showed a few minor sliding cracks, which are attributed to thermal fatigue. Consequently, all of these wear types on the pads' contact surface exhibit minimal effects, as indicated by SEM analysis and EDX mapping. Similarly, the compositions of sample S1 and sample S2 changed significantly after the friction test. The composition of the 'C' element increased in both samples, while the oxide compositions experienced slight changes following use. Additionally, due to friction and wear, most elements' weight percentage compositions altered, as presented in Table 11.

Table 11. Weight percentage of composition S1 and S2 after the friction test.

S1 After test			S2 After test		
Element	Weight %	Atomic %	Element	Weight %	Atomic %
C K	50.6	63.5	C K	35.5	47.7
O K	32.4	30.5	O K	40.3	40.7
MgK	1.2	0.7	MgK	1.6	1.1
AlK	2.2	1.2	AlK	4.2	2.5
SiK	4.2	2.3	SiK	10.6	6.1
MoL	4.5	0.7	MoL	3.5	0.6
CaK	1	0.4	CaK	2.7	1.1
BaL	2.2	0.2	BaL	1	0.1
FeK	1.7	0.4	FeK	0.5	0.1

In a nutshell, the following advantages can be enumerated from the proposed methodology:

- The mechanical, physical, and tribological performance of the samples has been reported, allowing for extensive analysis to draw definitive conclusions.
- Previous literature on brake friction materials (BFM) incorporating both rice husk (RH) and sugarcane bagasse ash (SCBA) has not addressed the fade and recovery performance, nor the worn-out surface morphology.
- This study effectively demonstrates the practicality of using brass and agricultural waste to create environmentally friendly brake pad friction materials.

5. CONCLUSIONS AND FUTURE SCOPE

This research on the utilization of agricultural waste, specifically rice husk (RH) and sugarcane bagasse ash (SCBA), in brake friction materials (BFM) aimed to address the issue of waste management for these by-products. Additionally, there has been an effort to eliminate hazardous compounds such as copper and asbestos in friction materials. By examining the physical, mechanical, and tribological properties, the following conclusions were drawn:

- The findings of this study indicate that copper can be replaced with various alternatives, including brass, alumina, and graphite. The weight percentage of brass used was 2%. However, increasing the percentage of brass can stabilize friction, enhance heat conductivity, and improve tribological characteristics, although it will also increase the density of the friction material [14].
- The densities recorded for samples S1 and S2 were 2.00 and 1.98 g/cc, respectively. The increased density is primarily attributed to the higher filler content, which enhances the homogeneity of the composite brake pad.
- Mechanical tests demonstrated that the results of the compression, tension, shear, and flexure tests are comparable to those of commercial brake pads and previous studies.
- Sample S1, with a higher weight percentage of rice husk, exhibited lower shear strength compared to a commercial brake pad. In contrast, sample S2 had a higher weight percentage of SCBA, which improved the bonding of the particles with the binder during the molding process.
- The coefficient of friction (COF) referenced in the literature for automotive applications ranges from 0.3 to 0.7. The fade COF for S1 and S2 during the first cycle did not differ significantly, even after the composites were subjected to temperatures of 289°C and 345°C during the first and second fade cycles, respectively. There was no significant change in fading under various conditions, making these materials suitable for vehicle applications.
- In the fade and recovery test, both S1 and S2 demonstrated fade resistance and recovery percentages that meet the necessary requirements.
- The wear mass percentages for S1 and S2 were calculated at 11.32 and 11.11, respectively. Although S1 exhibited higher hardness, its wear was slightly greater than that of S2. This increased wear in S1 is attributed to the higher weight percentage of rice husk, leading to fiber debonding from the base material during testing.
- Scanning Electron Microscopy with Energy Dispersive X-ray Spectroscopy (SEM-EDX) analysis indicated that the matrix was well-bonded, the material was uniformly distributed, there was no fiber delamination, and tribofilm formation contributed to maintaining stable friction.

This study has demonstrated that rice husk (RH) and sugarcane bagasse ash (SCBA) can be effectively used to produce environmentally friendly brake pads. Additionally, utilizing agricultural waste in industrial applications appears to be a promising approach. Based on the findings of this research, several areas for future investigation are suggested.

- Mechanical and tribological tests were performed without statistical error analysis; future studies should include replicates and measures of uncertainty.

- Further investigation is necessary regarding particulate emissions (PM) and the potential for silica crystallization during high-temperature braking.
- There is potential for optimizing the percentage of RH and SCBA, along with processing parameters, to reduce wear without sacrificing strength.
- The impact of varying brass percentages on wear estimation warrants analysis, as existing literature indicates that brass content should be maintained between 4.5% and 8%.
- The numerical analysis in the literature has indicated that applied pressure, pad penetration, and its temperature are connected to each other. During prolonged braking, the temperature can go up to 800^{0}C, causing excessive fade. So, the thermal conductivity and heat capacity of BFM can be investigated [77].

REFERENCES

[1] A. Belhocine, D. Shinde, and R. Patil, "Thermo-mechanical coupled analysis-based design of ventilated brake disc using genetic algorithm and particle swarm optimization," *JMST Adv*ances, vol. 3, no. 3, pp. 41–54, Jun. 2021, doi: 10.1007/s42791-021-00040-0.

[2] H. P. Khairnar, V. M. Phalle, and S. S. Mantha, "Comparative frictional analysis of automobile drum and disc brakes," *Tribol. Ind*., vol. 38, no. 1, pp. 11–23, Mar. 2016.

[3] K. L. Sundarkrishnaa, *Friction Material Composites: Copper-/Metal-Free Material Design Perspective*, in Springer Series in Materials Science, Cham: Springer International Publishing, 2015. doi: 10.1007/978-3-319-14069-8.

[4] G. Gautier Di Confiengo and M. G. Faga, "Ecological Transition in the Field of Brake Pad Manufacturing: An Overview of the Potential Green Constituents," *Sustainability*, vol. 14, no. 5, p. 2508, Feb. 2022, doi: 10.3390/su14052508.

[5] V. Chaudhary and F. Ahmad, "A review on plant fiber reinforced thermoset polymers for structural and frictional composites," *Polymer Testing*, vol. 91, p. 106792, Aug. 2020, doi: 10.1016/j.polymertesting.2020.106792.

[6] V. Mahale, J. Bijwe, and S. Sinha, "A step towards replacing copper in brake-pads by using stainless steel swarf," *Wear*, vol. 424–425, pp. 133–142, Feb. 2019, doi: 10.1016/j.wear.2019.02.019.

[7] M. Amirjan, "Microstructure, wear and friction behavior of nanocomposite materials with natural ingredients," *Tribol. Int*., vol. 131, pp. 184–190, Oct. 2018, doi: 10.1016/j.triboint.2018.10.040.

[8] D. L. Singaravelu, R. Vijay, and P. Filip, "Influence of various cashew friction dusts on the fade and recovery characteristics of non-asbestos copper free brake friction composites," *Wear*, vol. 426–427, pp. 1129–1141, Apr. 2019, doi: 10.1016/j.wear.2018.12.036.

[9] P. W. Lee and P. Filip, "Friction and wear of Cu-free and Sb-free environmental friendly automotive brake materials," *Wear*, vol. 302, no. 1–2, pp. 1404–1413, Jan. 2013, doi: 10.1016/j.wear.2012.12.046.

[10] K. Asrar Ahmed, S. Rasool Mohideen, S. R. Balachandran, and M. A. Sai Balaji, "Varying Cu and Zn composition in brass and its effect on the fade and recovery behavior of the phenolic-based friction composites," *Polym. Compos*., vol. 43, no. 7, pp. 4478–4494, Jul. 2022, doi: 10.1002/pc.26706.

[11] M. Kchaou, A. Sellami, A. R. Abu Bakar, A. R. Mat Lazim, R. Elleuch, and S. Kumar, "Brass fillers in friction composite materials: Tribological and brake squeal characterization for suitable effect evaluation," *Steel Compos. Struct*., vol. 19, no. 4, pp. 939–952, Oct. 2015, doi: 10.12989/scs.2015.19.4.939.

[12] K. A. Ahmed, S. R. Mohideen, M. A. S. Balaji, and B. S. Rajan, "Tribological performance of brass powder with different copper and zinc content in the brake pad," *Tribol. Ind*., vol. 42, no. 2, pp. 177–190, 2020, doi: 10.24874/ti.783.10.19.03.

[13] A. Sellami, M. Kchaou, R. Kus, J. Fajoui, R. Elleuch, and F. Jaquemin, "Impact of brass contents on thermal, friction and wear properties of brake linings composites," *Mech. Ind*., vol. 19, no. 1, 2018, doi: 10.1051/meca/2016083.

[14] J. Bijwe, M. Kumar, P. V. Gurunath, Y. Desplanques, and G. Degallaix, "Optimization of brass contents for best combination of tribo-performance and thermal conductivity of non-asbestos organic (NAO) friction composites," *Wear*, vol. 265, no. 5–6, pp. 699–712, Aug. 2008, doi: 10.1016/j.wear.2007.12.016.

[15] N. Stojanovic, A. Belhocine, O. I. Abdullah, and I. Grujic, "The influence of the brake pad construction on noise formation, people's health and reduction measures," *Environmental Science and Pollution Research*, vol. 30, no. 6, pp. 15352–15363, Sep. 2022, doi: 10.1007/s11356-022-23291-3.

[16] D. Lenin Singaravelu, R. Vijay, and M. Rahul, "Influence of Crab Shell on Tribological Characterization of Eco-Friendly Products Based Non Asbestos Brake Friction Materials," *SAE Technical Papers on CD-ROM/SAE Technical Paper Series*, vol. 1, Sep. 2015, doi: 10.4271/2015-01-2676.

[17] Y. Liu *et al*., "Evaluation of wear resistance of corn stalk fiber reinforced brake friction materials prepared by wet granulation," *Wear*, vol. 432–433, p. 102918, Jun. 2019, doi: 10.1016/j.wear.2019.05.033.

[18] T. Singh, C. I. Pruncu, B. Gangil, V. Singh, and G. Fekete, "Comparative performance assessment of pineapple and Kevlar fibers based friction composites," *Journal of Materials Research and Technology*., vol. 9, no. 2, pp. 1491–1499, Dec. 2019, doi: 10.1016/j.jmrt.2019.11.074.

[19] H. Sosiati, Y. A. Shofie, and A. W. Nugroho, "Tensile properties of Kenaf/E-glass reinforced hybrid polypropylene (PP) composites with different fiber loading," *Evergreen*, vol. 5, no. 2, pp. 1–5, 2018, doi: 10.5109/1936210.

[20] K. K. Ikpambese, D. T. Gundu, and L. T. Tuleun, "Evaluation of palm kernel fibers (PKFs) for production of asbestos-free automotive brake pads," *J. King Saud Univ. - Eng. Sci.,* vol. 28, no. 1, pp. 110–118, 2016, doi: 10.1016/j.jksues.2014.02.001.

[21] A. O. A. Ibhadode and I. M. Dagwa, "Development of asbestos-free friction lining material from palm kernel shell," *J. Brazilian Soc. Mech. Sci. Eng*., vol. 30, no. 2, pp. 166–173, Mar. 2008, doi: 10.1590/s1678-58782008000200010.

[22] Z. Fu *et al.,* "Development of eco-friendly brake friction composites containing flax fibers," *J. Reinf. Plast. Compos*., vol. 31, no. 10, pp. 681–689, 2012, doi: 10.1177/0731684412442258.

[23] P. I. Purboputro, M. A. Hendrawan, and A. Hariyanto, "Use of bamboo fiber as a brake pad lining material and the influence of its portion on hardness and durability," *IOP Conference Series Materials Science and Engineering*, vol. 403, p. 012100, Oct. 2018, doi: 10.1088/1757-899X/403/1/012100.

[24] N. Kumar, S. Kumar, J. S. Grewal, V. Mehta, and S. Ali, "Comparative study of Abaca fiber and Kevlar fibers based brake friction composites," *Polym. Compos*., vol. 43, no. 2, pp. 730–740, 2022, doi: 10.1002/pc.26405.

[25] I. Lawan, H. Argunam, M. Okhawilai, C. H. Ahn, and S. Rimdusit, "Bio-based treatment of hemp fiber for use as reinforcement of a composite: An effort towards development of green and sustainable polybenzoxazine brake pad," *Tribology International*, vol. 193, p. 109394, Feb. 2024, doi: 10.1016/j.triboint.2024.109394.

[26] M. A. Maleque and A. Atiqah, "Development and Charactrization of Coir Fibre Reinforced Composite Brake Friction Materials," *Arab. J. Sci. Eng*., vol. 38, no. 11, pp. 3191–3199, 2013, doi: 10.1007/s13369-012-0454-4.

[27] X. Xin, C. G. Xu, and L. F. Qing, "Friction properties of sisal fibre reinforced resin brake composites," *Wear*, vol. 262, no. 5–6, pp. 736–741, 2007, doi: 10.1016/j.wear.2006.08.010.

[28] W. Asotah and A. Adeleke, "Development of asbestos free brake pads using corn husks," *Leonardo Electron. J. Pract. Technol*., pp. 129–144, 2017.

[29] U. D. Idris, V. S. Aigbodion, I. J. Abubakar, and C. I. Nwoye, "Eco-friendly asbestos free brake-pad: Using banana peels," *J. King Saud Univ. - Eng. Sci*., vol. 27, no. 2, pp. 185–192, Jul. 2015, doi: 10.1016/j.jksues.2013.06.006.

[30] J. Chandradass, M. Amutha Surabhi, P. Baskara Sethupathi, and P. Jawahar, "Development of low cost brake pad material using asbestos free sugarcane bagasse ash hybrid composites," *Materials Today Proceedings*, vol. 45, pp. 7050–7057, Jan. 2021, doi: 10.1016/j.matpr.2021.01.877.

[31] G. S. Gehlen, P. D. Neis, L. Y. Barros, J. C. Poletto, N. F. Ferreira, and S. C. Amico, "Tribological performance of eco-friendly friction materials with rice husk," *Wear*, vol. 500–501, p. 204374, May 2022, doi: 10.1016/j.wear.2022.204374.

[32] D. Carlevaris, M. Leonardi, G. Straffelini, and S. Gialanella, "Design of a friction material for brake pads based on rice husk and its derivatives," *Wear*, vol. 526–527, Aug. 2023, doi: 10.1016/j.wear.2023.204893.

[33] R. Mathur and V. K. Srivastava, "Crop Residue Burning: Effects on Environment," in Energy, Environment, and Sustainability, 2018, pp. 127–140. doi: 10.1007/978-981-13-3272-2_9.

[34] N. Jain, A. Bhatia, and H. Pathak, "Emission of air pollutants from crop residue burning in India," *Aerosol Air Qual. Res*., vol. 14, no. 1, pp. 422–430, 2014, doi: 10.4209/aaqr.2013.01.0031.

[35] K. Ravindra, T. Singh, and S. Mor, "Emissions of air pollutants from primary crop residue burning in India and their mitigation strategies for cleaner emissions," *J. Clean. Prod*., vol. 208, pp. 261–273, 2019, doi: 10.1016/j.jclepro.2018.10.031.

[36] A. R. Sharma, S. K. Kharol, K. V. S. Badarinath, and D. Singh, "Impact of agriculture crop residue burning on atmospheric aerosol loading - A study over Punjab State, India," *Ann. Geophys*., vol. 28, no. 2, pp. 367–379, 2010, doi: 10.5194/angeo-28-367-2010.

[37] B. Krishna, K. Balakrishnan, A. R. Siddiqui, B. A. Begum, D. Bachani, and M. Brauer, "Tackling the health burden of air pollution in South Asia," *BMJ*, vol. 359, p. j5209, Nov. 2017, doi: 10.1136/bmj.j5209.

[38] P. Ghosh, S. Sharma, and I. Khanna, "*Scoping Study for South Asia Air Pollution*," 2019. [Online]. Available: https://assets.publishing.service.gov.uk/media/5cf0f3b0e5274a5eb03386da/TERI_Scoping_Study_final_report_May27_2019.pdf. Accessed: Jun. 6, 2025.

[39] U.S. Department of Agriculture, "Prodcution - Rice," 2024, [Online]. Available: https://www.fas.usda.gov/data/production/commodity/0422110. Accessed: Jun. 6, 2025.

[40] "Top 10 sugarcane producing countries," *Current Affairs 2025 – Today's Latest Current Affairs*, 2025, [Online]. Available: https://currentaffairs.adda247.com/top-10-sugarcane-producing-countries-in-the-world/. Accessed: Jun. 6, 2025.

[41] R. N. Swamy, *Cement Replacement Materials (Concrete Technology and Design)*, Surrey University press, London UK, 1986.

[42] N. Stojanovic, J. Glisovic, O. I. Abdullah, A. Belhocine, and I. Grujic, "Particle formation due to brake wear, influence on the people health and measures for their reduction: a review," *Environ. Sci. Pollut. Res*., vol. 29, no. 7, pp. 9606–9625, 2022, doi: 10.1007/s11356-021-17907-3.

[43] N. Stojanovic, S. Igrutinovic, A. Belhocine, B. Boskovic, and I. Grujic, "The composition, working parameters and measures for the brake wear reduction: A review," *Proc. Inst. Mech. Eng. Part J J. Eng. Tribol*., vol. 239, no. 4, pp. 393–409, 2025, doi: 10.1177/13506501241291393.

[44] International Agency for Research on Cancer, "Agents classified by the IARC monographs," *Igarss*, vol. 1–105, no. 1, pp. 1–5, 2012.

[45] R. Merget *et al.,* "Health hazards due to the inhalation of amorphous silica," *Archives of Toxicology*, vol. 75, no. 11–12, pp. 625–634, Nov. 2001, doi: 10.1007/s002040100266.

[46] A. Belhocine, N. M. Ghazali, and O. I. Abdullah, "Structural and contact analysis of a 3-dimensional disc-pad model with and without thermal effects," *Tribol. Ind.,* vol. 36, no. 4, pp. 406–418, 2014.

[47] S. S. Barve and H. P. Khairnar, "Use of rice Husk and Sugarcane Bagasse Ash for Development of Automotive Brake Pad Friction Material," *Evergreen*, vol. 12, no. 1, pp. 27–40, 2025, doi: 10.5109/7342436.

[48] J. Bijwe, Nidhi, N. Majumdar, and B. K. Satapathy, "Influence of modified phenolic resins on the fade and recovery behavior of friction materials," *Wear*, vol. 259, no. 7–12, pp. 1068–1078, 2005, doi: 10.1016/j.wear.2005.01.011

[49] N. Stojanovic, A. Belhocine, O. Abdullah, I. Grujic, and M. Petrovic, "The influence of the cooling on the disc brakes temperature increment from the aspect of traffic safety," *Thermal Science*, vol. 29, no. 5 Part B, pp. 3887–3898, Jan. 2025, doi: 10.2298/tsci241102065s.

[50] Automotive Manufacturer Equipment Companies Agency, *Verhicle Equipment Safety Commission Regulation V-3 Test*, 1982.

[51] Bureau of Indian Standards, *Automotive Vehicles - Brake linings, Part 4: Co-efficient of Friction - Method of Test*, 1994.

[52] N. Elzayady and R. Elsoeudy, "Microstructure and wear mechanisms investigation on the brake pad," *Journal of Materials Research and Technology*, vol. 11, pp. 2314–2335, Feb. 2021, doi: 10.1016/j.jmrt.2021.02.045.

[53] S. P. Jadhav and S. H. Sawant, "A review paper: Development of novel friction material for vehicle brake pad application to minimize environmental and health issues," *Materials Today Proceedings*, vol. 19, pp. 209–212, Jan. 2019, doi: 10.1016/j.matpr.2019.06.703.

[54] J. Abutu, S. A. Lawal, M. B. Ndaliman, R. A. Lafia-Araga, O. Adedipe, and I. A. Choudhury, "Production and characterization of brake pad developed from coconut shell reinforcement material using central composite design," *SN Appl. Sci*., vol. 1, no. 1, Dec. 2018, doi: 10.1007/s42452-018-0084-x.

[55] G. Akincioğlu, S. Akincioğlu, H. Öktem, And İ. Uygur, "Brake Pad Performance Characteristic Assessment Methods," *Int. J. Automot. Sci. Technol*., vol. 5, no. 1, pp. 67–78, Mar. 2021, doi: 10.30939/ijastech..848266.

[56] N. A. Hooton, "Metal-Ceramic Composites in High- Energy Friction Applications," *Bend Tech J.*, pp. 55–61, 1969.

[57] A. R. Marewad DS, Singh, GP, "Asbestos free brake pad using Micro cellulose fibre for automotive industry," *Int. J. Adv. Res. ideas Innov. Technol.*, vol. 4, no. 4, pp. 685–690, 2018.

[58] A. V.S, U. Akadike, S. Hassan, F. Asuke, and J. Agunsoye, "Development of Asbestos - Free Brake Pad Using Bagasse," *Tribol. Ind.*, vol. 32, pp. 12–18, Mar. 2010.

[59] A. R. Farah Nordyana, A. Z. Romli, and M. H. Abidin, "Effect of rice husk particle size on tensile and density of recycled PPVC composite," *Advanced Materials Research*, vol. 812, pp. 145–150, Sep. 2013, doi: 10.4028/www.scientific.net/AMR.812.145.

[60] V. S. Aigbodion., U. Akadike, S.B. Hassan, F. Asuke, and J.O. Agunsoye, "Development of Asbestos-Free Brake Pad Using Bagasse," *Tribol. Ind.,* vol. 32, pp. 12–18, Mar. 2010.

[61] O. Adeyemi, N. Ademoh, and T. Boye, "Development of Asbestos-Free Automotive Brake Pad Using Ternary Agro-Waste Fillers," *J. Multidiscip. Eng. Sci. Technol.*, vol. 3, pp. 5307–5323, Jul. 2016.

[62] M. N. Joshi, "Disc brake linings-analytical study and selection criteria," *SAE Technical Papers on CD-ROM/SAE Technical Paper Series*, Jun. 1980, doi: 10.4271/800782.

[63] V. Roubicek, H. Raclavska, D. Juchelkova, and P. Filip, "Wear and environmental aspects of composite materials for automotive braking industry," *Wear*, vol. 265, no. 1–2, pp. 167–175, 2008, doi: 10.1016/j.wear.2007.09.006.

[64] M. Eriksson and S. Jacobson, "Tribological surfaces of organic brake pads," *Tribol. Int.*, vol. 33, no. 12, pp. 817–827, 2000, doi: 10.1016/S0301-679X(00)00127-4.

[65] D. L. Singaravelu, R. Vijay, and P. Filip, "Influence of various cashew friction dusts on the fade and recovery characteristics of non-asbestos copper free brake friction composites," *Wear*, vol. 426–427, pp. 1129–1141, Apr. 2019, doi: 10.1016/j.wear.2018.12.036.

[66] N. Stojanovic, A. Belhocine, O. Abdullah, Z. Djuric, and I. Grujic, "Numerical Determination Of The Heating And Wear Of Brake Pads On The Basis Of Experimental Researches," in *Proceedings - 19th International Conference on Tribology - SERBIATRIB '25*, Faculty of Engineering University of Kragujevac, Serbia, May 2025. doi: 10.24874/ST.25.109.

[67] G. Straffelini, *Friction and Wear: Methodologies for Design and Control*. in Springer Tracts in Mechanical Engineering. Cham: Springer International Publishing, 2015. doi: 10.1007/978-3-319-05894-8.

[68] M. Naidu, A. Bhosale, Y. Munde, S. Salunkhe, and H. M. A. Hussein, "Wear and Friction Analysis of Brake Pad Material Using Natural Hemp Fibers," *Polymers*, vol. 15, no. 1, p. 188, Dec. 2023, doi: 10.3390/polym15010188.

[69] T. Mandziy *et al.*, "Evaluation of the Degree of Degradation of Brake Pad Friction Surfaces Using Image Processing," *Lubricants*, vol. 12, no. 5, p. 172, May 2024, doi: 10.3390/lubricants12050172.

[70] S. Babu, N. S. Kumar, M. Athar, and Y. Mani, "A Study of Braking Materials , Their Testing and Analysis," *Jr. Ind. Pollut. Control*, vol. 33, no. 2, pp. 1655–1658, 2017.

[71] P. Kosbe, P. Patil, and R. Kulkarni, "Fade and recovery characteristics of commercial disc brake friction materials: a case study," *Int. J. Ambient Energy*, vol. 43, no. 1, pp. 2446–2452, 2022, doi: 10.1080/01430750.2020.1730959.

[72] I. S. Tania and M. Ali, "Utilization of titanium dioxide (TiO2) nanoparticles to improve functionality and mechanical performances of cotton fabric," *Heliyon*, vol. 10, no. 18, p. e37899, 2024, doi: 10.1016/j.heliyon.2024.e37899.

[73] P. Babu and D. G. Solomon, "Case studies on characterization of brake pad surfaces using scanning electron microscope," *Malaysian J. Microsc.*, vol. 17, no. 1, pp. 111–122, 2021.

[74] S. Kumar and S. K. Ghosh, "Porosity and tribological performance analysis on new developed metal matrix composite for brake pad materials," *J. Manuf. Process.*, vol. 59, pp. 186–204, Sep. 2020, doi: 10.1016/j.jmapro.2020.09.053.

[75] J. R. Laguna-Camacho *et al.,* "A study of the wear mechanisms of disk and shoe brake pads," *Eng. Fail. Anal.*, vol. 56, pp. 348–359, Jan. 2015, doi: 10.1016/j.engfailanal.2015.01.004.

[76] M. Mor *et al.,* "Tribological behavior of carbon fiber reinforced ZrB2 based ultra high temperature ceramics," *J. Eur. Ceram. Soc.*, vol. 43, no. 13, pp. 5413–5424, 2023, doi: 10.1016/j.jeurceramsoc.2023.05.019.

[77] N. Stojanović, O. I. Abdullah, J. Schlattmann, I. Grujić, and J. Glišović, "Investigation of the penetration and temperature of the friction pair under different working conditions," *Tribology in Industry*, vol. 42, no. 2, pp. 288–298, Jun. 2020, doi: 10.24874/ti.849.02.20.05.

NOMENCLATURE:

BFM	Brake pad friction material
RH	Rice Husk
SCBA	Sugarcane Bagasse ash
SEM	Scanning Electron Microscopy
EDX	Energy Dispersive X-ray Spectroscopy
S1	Sample 1
S2	Sample 2
PM	Particulate matter
COF	Coefficient of Friction